Engineering Structures 111 (2016) 48–63

Contents lists available at ScienceDirect

Engineering Structures

journal homepage: www.elsevier.com/locate/engstruct

Experimental evaluation of out-of-plane capacity of masonry infill walls

André Furtado [a], Hugo Rodrigues [b,*], António Arêde [a], Humberto Varum [a]

[a] CONSTRUCT – LESE, Department of Civil Engineering, Faculty of Engineering, University of Porto, Portugal
[b] RISCO – School of Technology and Management, Polytechnic Institute of Leiria, Portugal

ARTICLE INFO

Article history:
Received 9 September 2015
Revised 16 November 2015
Accepted 11 December 2015
Available online 5 January 2016

Keywords:
Infill masonry walls
Out-of-plane behaviour
In-plane behaviour
Hysteretic behaviour
Damage evolution
Energy dissipation

ABSTRACT

Infill masonry (IM) walls are considered to be non-structural elements but, when subjected to earthquakes, they tend to interact with the surrounding RC (reinforced concrete) frames, which can result in different failure modes depending on the combination of the in-plane and out-of-plane behaviour. Therefore, the contribution of IM panels should be considered in the structural response analysis of existing buildings, for which an understanding of the out-of-plane non-linear behaviour of IM walls is of paramount importance in order to develop efficient strengthening solutions to prevent collapse and improve their performance in future earthquakes, and consequently reduce their seismic vulnerability. In order to obtain further knowledge of the out-of-plane response of IM panels, a study of full-scale IM walls was carried out with the realization of three experimental (cyclic and monotonic) out-of-plane tests with and without previous in-plane damage. The experiments, material characterization and the test set-up will be described in this paper as well as presenting and discussing the main test results, namely in terms of hysteretic force–displacement curves, damage evolution, stiffness degradation and energy dissipation.

1. Introduction

In recent years, interest has increased in the study of infill masonry (IM) walls, namely in their influence on the seismic response of existing buildings. The contribution of the presence of IM to a building's seismic performance can be favourable or unfavourable, depending on a series of phenomena detailing aspects and mechanical properties, such as the relative stiffness and strength between the frames and the IM walls, and the type of connection between the IM and the structures [1–7].

From the surveys of damaged and collapsed reinforced concrete (RC) buildings in recent earthquakes, a large number of buildings that suffered severe damage or collapse had their poor performance associated with the influence of the infill panels [8,9]. In some RC buildings subjected to seismic actions it is possible to observe that the major part of the structural elements has satisfactory behaviour with slight or no damage; however, their IM walls suffer much damage (in-plane or out-of-plane). Detachment of the IM panel from the surrounding RC frame, diagonal cracking as well as sliding cracking in the centre of the panel, shown in Fig. 1a–c are frequently observed.

Moreover, the non-balanced in-plane distribution of infill panels can introduce global torsion in buildings, which can induce larger demands on columns that were not considered in the original design [10–12].

Three main mechanisms associated with the presence of IM walls have been reported. One is associated with the short column mechanism, where IM walls leave a short portion of the column clear, concentrating larger demands in a short element; another is related to the absence of panels on the ground floor, inducing a sudden change in the storey stiffness and strength in height, leading to a soft-storey mechanism [13]. The third and one of the most critical failures is the out-of-plane infill, illustrated in Fig. 2. One of the major factors that causes out-of-plane instability and poor performance is the deficient/insufficient support-width of the RC beams and/or slabs, normally adopted to minimize the thermal-bridge effect, with no connection between the interior and the exterior panels and, finally, no connection to the surrounding RC frames [9,14].

It is consensual that further and deeper knowledge is required of the out-of-plane behaviour of IM walls to develop effective retrofit strategies that prevent this type of collapse and consequently protect the buildings' users' safety, as well as that of people near the building. The study of this type of collapse mechanism is also important to support the development of accurate numerical models that represent the expected behaviour of IM walls subjected to out-of-plane loadings, combined or not with in-plane loadings.

Thus, the experimental test appears to be an excellent tool that allows the study of IM walls subjected to static or dynamic cyclic

* Corresponding author. Tel.: +351 244 843351.
E-mail address: hugo.f.rodrigues@ipleiria.pt (H. Rodrigues).

http://dx.doi.org/10.1016/j.engstruct.2015.12.013
0141-0296/

Fig. 1. Typical damage observed on in-plane IM walls: (a) detachment of the surrounding RC frame in the L'Aquila (Italy) earthquake, (b) diagonal cracking in Lorca (Spain) and (c) in the Nepal earthquake.

Fig. 2. IM walls out-of-plane collapse: (a) and (b) in the L'Aquila earthquake, and (c) in the Nepal Earthquake in 2015.

experimental tests combining different types of test variation, such as: evaluation of the out-of-plane performance with different in-plane damage levels, variations in the dimensions of the IM walls, and different types of masonry bricks. However this type of experimental test is difficult to perform as it requires complex experimental set-ups with sufficient capacity for large samples. Some experimental studies have been carried out in order to characterize the out-of-plane performance of the infill panels considering and ignoring previous in-plane damage [15–17]. It was observed that the out-of-plane capacity of the IM walls is reduced with the increase in in-plane demands, leading to the conclusion that further experimental investigations, mainly of specimens representative of the country's building stock, are of extreme importance.

From previous works and based also on the results provided by the experimental tests some important direction can be withdrawn for the future, and in particular can be fundamental to earthquake prone countries, namely: (i) the structural engineers should take into account with the structural contribution of this non-structural elements in the buildings response when subjected to earthquake loadings; (ii) With the experimental characterization of the IM walls it is possible to develop some strengthening strategies that could reduce their vulnerability, and thus save people's lives and decrease the level of damages that this non-structural elements are subjected to; (iii) new guidelines regarding the IM walls construction process can be drawn to improve their seismic performance, and thus eliminate some factors that increase their in-plane and/or out-of-plane seismic vulnerability (such for example construction of infill panels disconnected of the surrounding RC frame, etc.); (iv) The experimental data results can be used to calibrate numerical models, and thus assess the seismic vulnerability of existing and/or new buildings considering the IM walls real and expected behaviour when subjected to an earthquake.

Based on this motivation, an experimental campaign was undertaken with the main goal of characterizing the out-of-plane behaviour of infilled RC frames. Full-scale experimental tests were undertaken at the Laboratory of Earthquake and Structural Engineering – LESE, with the geometry based on a previous statistical study conducted into Portuguese RC building stock, namely buildings constructed in the 1960s and 1970s [18]. The results of the experiments comprising three out-of-plane tests (with and without previous in-plane damage) will be presented and also discussed in terms of hysteretic force–displacement curves, damage evolution, cracking pattern and displacements profiles.

2. Experimental tests

2.1. Experimental tests overview and specimen descriptions

The present experiments comprised three out-of-plane tests of full-scale infilled RC frames, two of them without previous in-plane damage and one with previous in-plane damage. The general dimensions of the specimens were selected as 4.80 × 3.30 m and the cross sections of the RC columns and beams were 0.30 × 0.30 m and 0.30 × 0.50 m, respectively, which are representative of those existing in the Portuguese building stock [18]. Fig. 3 shows the RC infilled frame geometry, as well as the corresponding

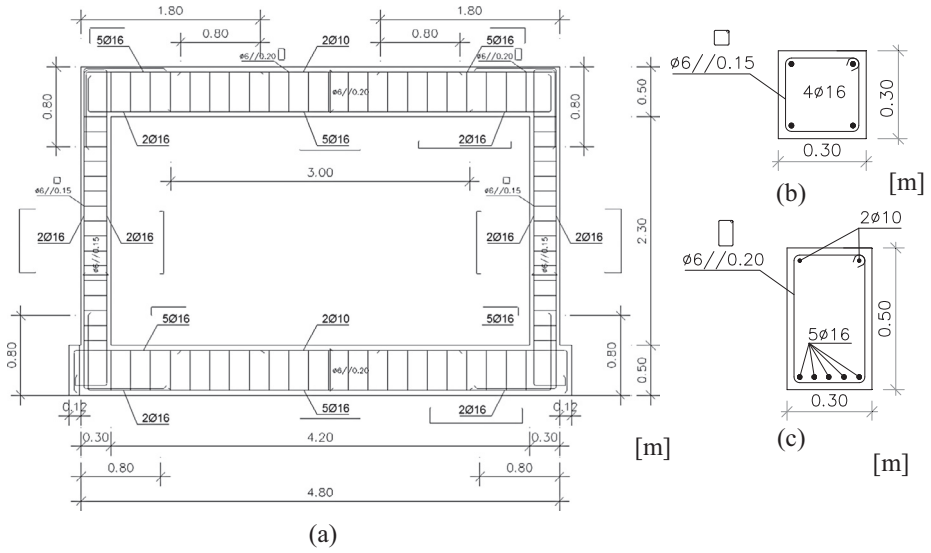

Fig. 3. Infilled RC frame specimen dimensions (in m): (a) general dimensions, (b) column and (c) beam dimensions and reinforcement detailing.

column and beam dimensions and reinforcement detailing (Fig. 3b and c).

All infill panels have equal geometry with in-elevation dimensions of 2.30 × 4.20 m made of horizontal hollow clay bricks, as usually found in the most common masonry in Portugal. No reinforcement was used to connect the infill panel and the surrounding RC frame. Three infill panels were built (denoted as Inf_01, Inf_02 and Inf_03), all having an external leaf (150 mm thick) aligned with the external side of the RC beam. For the panel Inf_03, an internal leaf, 110 mm thick, was added aligned with internal side of the beam, leaving a hollow thickness of 40 mm. This double-leaf panel was first tested for in-plane cyclic displacements, after which the internal leaf was removed, leaving the external leaf to be tested under the same out-of-plane loading conditions as for panel Inf_02. A summary of the experimental tests and corresponding main characteristics are illustrated in Table 1.

2.2. Material characterization

2.2.1. Concrete and re-bar properties

The material ordered for the RC frame specimen construction consisted of regular C20/25-class concrete [19]. Considering a correction factor of 0.8 to convert (approximately) the mean cubic compressive strength, the yield is $f_{cm,cyl}$ = 21.4 MPa. Then, assuming the approximate relation $f_{ck,cyl} = f_{cm,cyl} - 8$ MPa, which estimates the characteristic value of the compressive strength, $f_{ck,cyl}$ = 13.4 MPa is obtained. Table 2 summarizes the results of the corresponding compression tests for concrete strength and elasticity modulus determination.

For the RC frame specimen construction, three different bar diameters were used, from the same lot, namely 6 mm, 10 mm and 16 mm. Three samples of each were taken from each diameter bar and tested according to [20]. The relevant results obtained are summarized in Table 3, in terms of Young's modulus, yield strength, ultimate strength and ultimate strain, for each sample and for the corresponding average value of each bar diameter.

2.2.2. Masonry properties

The RC frame was tested with three fully infilled specimens (Inf_01, Inf_02 and Inf_03). The selected masonry typology represents the common clay blocks used in Southern Europe with horizontal perforations and the geometric properties illustrated in Fig. 4. Two different brick typologies were adopted, varying only in the brick thickness. For the specimens Inf_01 and Inf_02 brick type A was used, and for Inf_03 both brick type A and brick type B were used with type B removed for the out-of-plane test.

A traditional mortar type M5 (*Ciarga*) was considered a suitable choice with respect to the normal practice of the Portuguese construction industry in the 1970s. The panels were constructed after the full hardening of the RC frame. The thickness of both the adopted vertical and the horizontal bed joints was 1 cm. Full contact between the infill panel and the surrounding RC elements was considered to be achieved by filling the vertical gaps between the infill and the top horizontal gap with mortar. Flexure and compressive mortar tests were carried out according to EN 196-2006, six samples for each panel. The main results are summarized in Table 4.

Further characterization tests were carried out on the mechanical properties of the IM wallets of each type of masonry brick. For this, seven samples (four of type A bricks and three of type B bricks) were subjected to vertical compression strength tests and six samples (three of each brick type) to diagonal compression

Table 1
Summary of the experimental tests and target maximum displacements.

Test number	Previous in-plane drift (%)	Axial load (kN)	Out-of-plane target displacement (mm)	Type	Number of leaves	Brick unit size $l \times h \times t$ (mm) 
Inf_01	–	300	70	Fully infilled	1	300 × 200 × 150
Inf_02	–				1	300 × 200 × 150
Inf_03	0.5%				2[a]	300 × 200 × 150 (ext.) 300 × 200 × 110 (int.)

[a] Only for in-plane testing prior to out-of-plane, for which the internal leaf was removed.

Table 2
Results from compression tests and elasticity modulus determination tests on concrete specimens according to NP-EN206 2000 [19].

Sample	Compressive ultimate strength fcu (MPa)	Average	SD[a]	COV[b]	Elasticity modulus $E_{c,cil}$ (GPa)	Average	SD[a]	COV[b]
1	26.3	26.8	2.108	0.08	24.5	24.7	0.79	0.03
2	28.8				24.3			
3	26.8				24.1			
4	28.2				26.0			
5	27.7				25.3			
6	22.9				24.0			

[a] Standard deviation.
[b] Coefficient of variation.

Table 3
Results from tensile tests on steel bar specimens according to NP-EN10002-1 2006 [20].

Diameter group (mm)	Sample	Young's modulus E (GPa)	Yield strength F_{sy} (MPa)	Ultimate strength F_{su} (MPa)	Ultimate strain ε_{su} (%)
6	1	208.7	450.3	570.5	16.2
	2	205.3	441.5	619.9	17.7
	3	198.5	440.3	589.1	15.3
	Average	204.2	444.0	593.2	16.4
10	1	207.1	586.3	680.8	20.7
	2	214.0	619.7	721.5	18.1
	3	207.9	590.8	692.3	20.8
	Average	209.7	598.9	698.2	19.9
12	1	203.7	492.8	616.6	26.9
	2	212.4	510.5	632.5	24.6
	3	212.2	479.8	595.9	27.2
	Average	209.4	494.4	615.0	26.2

tests, as illustrated in Fig. 5a and b respectively. The most common damage observed was top or bottom crushing and diagonal cracking of the wallets subjected to vertical compression strength tests and diagonal compression tests, and both types of representative damage are illustrated in Fig. 6a and b respectively.

Vertical compressive strength of $f_{m,A} = 0.531$ MPa and $f_{m,B} = 0.667$ MPa was obtained for wallets of brick types A and B, respectively, together with vertical elasticity modulus of $E_{m,A} = 1417.6$ MPa and $E_{m,B} = 3116.3$ MPa. The tests results are summarized in Table 5.

Diagonal compressive strength of $f_{md,A} = 0.303$ MPa and $f_{md,B} = 0.346$ MPa was obtained for wallets of brick types A and B respectively. The tests results are summarized in Table 6.

2.3. Modal identification

In order to determine the natural frequencies and the modal response of the IM wall, a series of vibration tests was performed before beginning the other tests. Among other interesting outputs, the modal analysis of the specimens led to different conclusions regarding some of their main mechanical properties in a non-tested state (for example the elastic modulus). The goal of the following measurements consisted of identifying the first natural frequencies and corresponding mode shapes of the masonry specimens. This dynamic identification allows calibration of the numerical models, and may be particularly important to engineers in practice when dealing with existing RC buildings with IM walls.

The measurements of the dynamic behaviour of the masonry walls were taken using LabVIEW Signal Express software [21] to log the data acquired from nine unidirectional accelerometers (see Fig. 7a) in time frames of approximately 15 min, excited with ambient noise vibration. The disposition of the accelerometers was found to be at the quarters of each dimension (3 accelerometers in each longitudinal and transversal direction) of the panel. The measurements were taken at a time when the set-ups for the out-of-plane tests were already assembled.

Modal analysis of the specimens was subsequently carried out by means of the peak picking and frequency domain decomposition (FDD) techniques, implemented in the ARTeMIS Extractor software [22], from which the first natural frequency of every single wall was of 24.31 Hz for the 15 cm thick panels (illustrated red in the Fig. 8 and the corresponding vibration mode can be observed in Fig. 7b) and about 31 Hz for the 11 cm thick panels. Additionally, a spectral peak is observed about 4 Hz which corresponds to the first out-of-plane frequency of the RC frame (illustrated black in Fig. 8).

3. Monotonic and cyclic out-of-plane experimental test of a full-scale im wall

The experimental characterization of the out-of-plane behaviour of IM walls was initially undertaken by comparing two IM walls subjected to monotonic out-of-plane loading (Inf_01) and cyclic out-of-plane loading (Inf_02). Additionally, axial load of 300 kN was applied to the infilled RC frame, Inf_01, in the RC column before the test. Thus, the influence of axial load in the RC

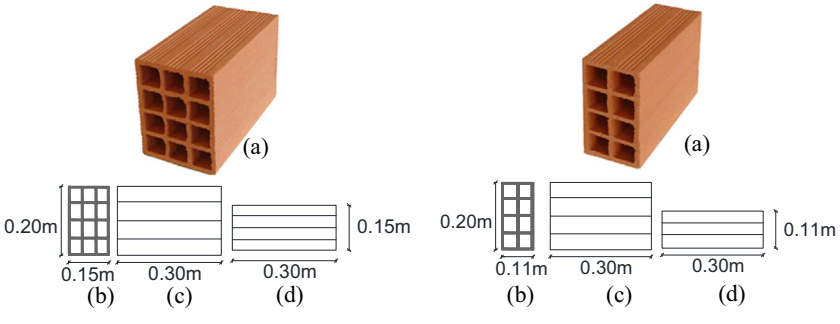

Fig. 4. Brick type geometric dimensions (in m): (a) brick general view, (b) front dimensions, (c) lateral dimensions and (d) upper dimensions.

Table 4
Results from flexure and compressive strength tests on mortar specimens.

Infill series test	Flexure strength (MPa)	Compressive strength (MPa)
Inf_01	5.65	16.55
Inf_02	2.11	5.66
Inf_03	4.27	13.40

columns in the response of the IM wall was also evaluated. In this section the out-of-plane test set-up, instrumentation, loading condition and the main results regarding the out-of-plane tests of IM walls without previous in-plane damage will be presented.

3.1. Description of the out-of-plane test set-up

The out-of-plane test consisted of the application of a uniformly distributed surface load through a system composed of seven nylon airbags, reacting against a self-equilibrated steel structure, as shown in Figs. 9 and 10. The application of a uniform out-of-plane loading pretends (as was observed) to globally mobilize the out-of-plane response of the IM wall. In the literature similar out-of-plane load distribution adopted by other authors can be found [23,24].

This reaction structure is composed of five vertical and four horizontal alignments of rigidly connected steel bars, in front of which a vertical wooden platform is placed to resist the airbag pressure and transfer it to the steel reacting grid elements. Thus, 12 steel threaded rods, crossing the RC elements in previously drilled holes, were used to equilibrate the reaction force resulting from the pressure applied by the airbags in the infill panel. The steel rods were strategically placed to evaluate the load distribution throughout the entire infilled RC frame resorting to load cells attached to each rod, which allowed continuous measurement of the forces transmitted to the reaction structure to which the rods were directly screwed. On the other extremity of each tensioned rod, appropriate nuts and steel plates were used to anchor the rod and apply its reaction force to the concrete surface by uniformly distributed normal stresses, thus avoiding load concentration on the RC elements crossed by the rods.

In each column, the axial load was applied by means of a hydraulic jack inserted between a steel cap placed on the top of the column and an upper HEB steel shape, which, in turn, was connected to the foundation steel shape resorting to a pair of high-strength rods per column. Hinged connections were adopted between these rods and the top and foundation steel shapes; the axial load actually applied to the columns was continuously measured by load cells inserted between the jacks and the top of each column, which was paramount in performing the in-plane tests.

The pressure level inside the airbags was set by two pressure valves which were controlled according to the target and measured out-of-plane displacement of the central point of the infill panel (the control node and variable) continuously acquired during the tests using a data acquisition and control system developed in the National Instruments LabVIEW software platform [25]. Prior to the experiments, calibration of the whole system was undertaken; this consisted of comparing the sum of the load cell forces with the airbag pressure resultant force (the pressure multiplied by the theoretical loaded panel area), in order to obtain the variation of load distribution, i.e. indirectly the actually loaded area, with the increase in distance between the steel reaction structure and the surface loaded panel. This calibration was achieved by inserting a vertical wooden panel supported in wood beams reacting against the RC top and bottom beams, thus without involving the brick masonry panel.

3.2. Instrumentation

The instrumentation of the experimental tests comprised a total of 23 displacement transducers, among linear variable displacement transducers (LVDTs) and draw wire transducers (DWTs), as illustrated in Fig. 11 The transducers were divided into 3 different groups according to the corresponding measurement objective: (i) IM wall out-of-plane displacements (13 DWTs), (ii) out-of-plane rotation between the infill panel and the surrounding RC frame (8 LVDTs) and (iii) out-of-plane displacements of the RC frame (2 LVDTs).

3.3. Loading condition

As previously stated, the aim of the present experiments is to better understand the out-of-plane behaviour of IM walls, particularly when subjected to previous in-plane damage. In addition, the assessment of the influence of the RC column axial load application in the out-of-plane response was made possible by imposing an axial load of 300 kN on each RC column during the test on Inf_01 and no axial load during tests on Inf_02 and Inf_03. Inf_03, comprising a double-leaf panel (brick types A and B), was first subjected to an in-plane drift of 0.5%, and then the brick type B panel was removed and the damaged type A wall was subjected to out-of-plane loading.

The Inf_01 test was carried out by imposing monotonic increasing out-of-plane displacements in the IM panel. With regard to the Inf_02 and Inf_03 tests, cyclic out-of-plane displacements were

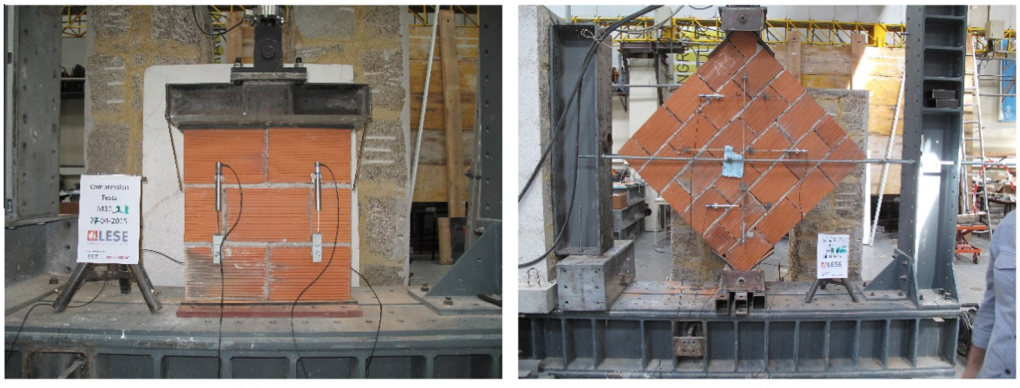

Fig. 5. Layout of the masonry wallet tests: (a) vertical compressive strength test and (b) diagonal tensile strength test.

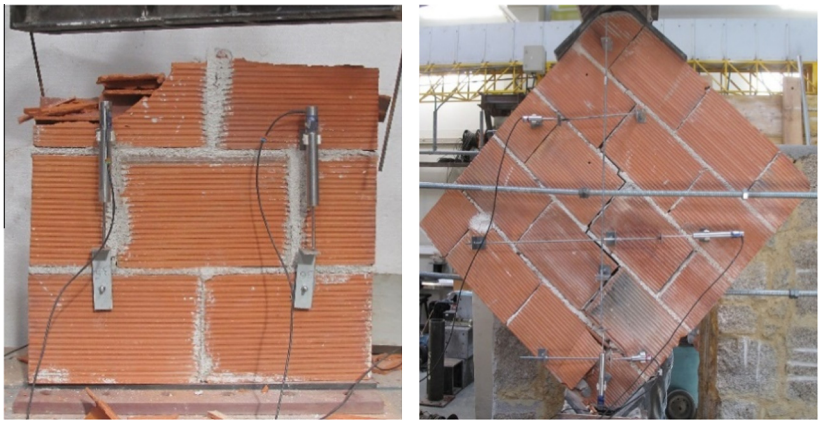

(a) (b)

Fig. 6. Masonry wallet damage after: (a) vertical compressive strength test and (b) diagonal tensile strength test.

Table 5
Results from compressive strength tests on IM wallet specimens.

Samples	$f_{m,I}$ (MPa)	E_i (MPa)
M_{A_1}	0.665	1826.1
M_{A_2}	0.524	1561.1
M_{A_3}	0.484	1047.8
M_{A_4}	0.447	1235.2
M_{B_1}	0.970	2595.4
M_{B_2}	0.758	4949.8
M_{B_3}	0.675	1803.8

Brick type	A		B	
Sample	$f_{m,I}$ (MPa)	E_i (MPa)	$f_{m,I}$ (MPa)	E_i (MPa)
Mean (MPa)	0.531	1417.6	0.801	3116.3
SD	0.095	345	0.152	1636
COV	0.18	0.24	0.189	0.53
Characteristic value (MPa)	0.442	–	0.667	–

Table 6
Results from the diagonal compressive strength tests on IM wallet specimens.

Samples	$f_{m,I}$ (MPa)
M_{A_1}	0.260
M_{A_2}	0.370
M_{A_3}	0.280
M_{B_1}	0.340
M_{B_2}	0.360
M_{B_3}	0.340

Brick type	A	B
Mean (MPa)	0.303	0.346
SD	0.059	0.012
COV	0.190	0.03

imposed on the IM wall with steadily increasing displacement levels, targeting the following nominal peak displacements: 2.5; 5; 7.5; 10; 15; 20; 25; 30; 35; 40; 45; 50; 50; 55; 60; 65 and 70 (mm), as illustrated in Fig. 12. Three cycles were repeated for each lateral deformation demand level at the control node chosen as the central point of the IM wall where concentrated deformation is expected.

3.4. Experimental test results

The main results of the out-of-plane tests of the fully infilled RC frames, Inf_01 and Inf_02, were evaluated in terms of shear-drift hysteretic curves, out-of-plane displacement profiles, damage evolution and crack pattern, stiffness and strength degradation, and energy dissipation.

3.4.1. Force–displacement hysteretic curves

From the force–displacement hysteretic curves in Fig. 13a and b, the following main observations can be drawn.

- The maximum strength was almost four times higher for the tests without previous in-plane damage (In_01 and Inf_02) and for higher out-of-plane drift values. For the Inf_01 and Inf_02 tests the maximum strength occurs for out-of-plane drift values of 1.5–2%.
- The strength degradation is particularly pronounced in both tests. This fact can be explained by the failure mode observed in this test (described below).
- By comparing Inf_01 and Inf_02, it was also verified that the initial stiffness of the IM walls was slightly affected by the axial loading in the RC columns. Namely, it was verified that the test with axial load (Inf_01) had about 5% more initial stiffness when compared with Inf_02.
- It was also verified that the initial cracking for the lower out-of-plane drift values for the Inf_02 was about 10%. The cracking force in both experimental tests was about 50 kN.

3.4.2. Damage evolution and cracking pattern

Aiming for a detailed observation of the damage evolution during the experimental tests, within the present study each test was stopped at the end of the last cycle of each displacement level in order to highlight and register new cracks and/or the evolution of existing cracks. Visual observation of the damage evolution during the tests yielded the information described in the following paragraphs. The final damage patterns of all tests are presented in Figs. 14 and 15, showing several differences between the tests with and without previous in-plane damage. The final cracking shape of Inf_01 was vertical, with detachment between the infill panel and the surrounding RC frame in the top and bottom joints, as shown in Figs. 14a and 15a. However, the Inf_02 test exhibited a trilinear cracking pattern with deformation concentrated in the mid-point of the wall, with slight cracking in the top joint, as illustrated in Figs. 14b and 15b.

3.4.3. Out-of-plane displacement profiles

The out-of-plane displacement profiles of both IM walls were measured during the experiment along three different alignments (a) left, (b) centre and (c) right and at five different heights ($h1 = 0$ m; $h2 = 1/3h_{wall}$; $h3 = 1/2h_{wall}$; $h4 = 2/3h_{wall}$ and $h5 = h_{wall}$,

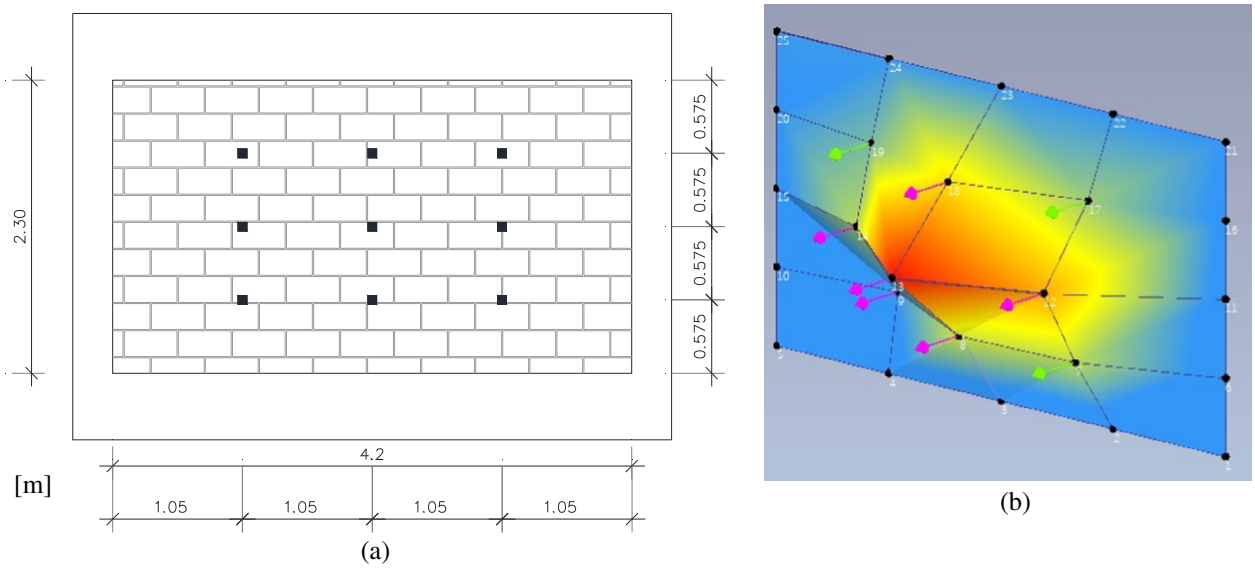

Fig. 7. Modal identification test: (a) layout of the test setup and location of the nine accelerometers (in m) and (b) first vibration mode shape.

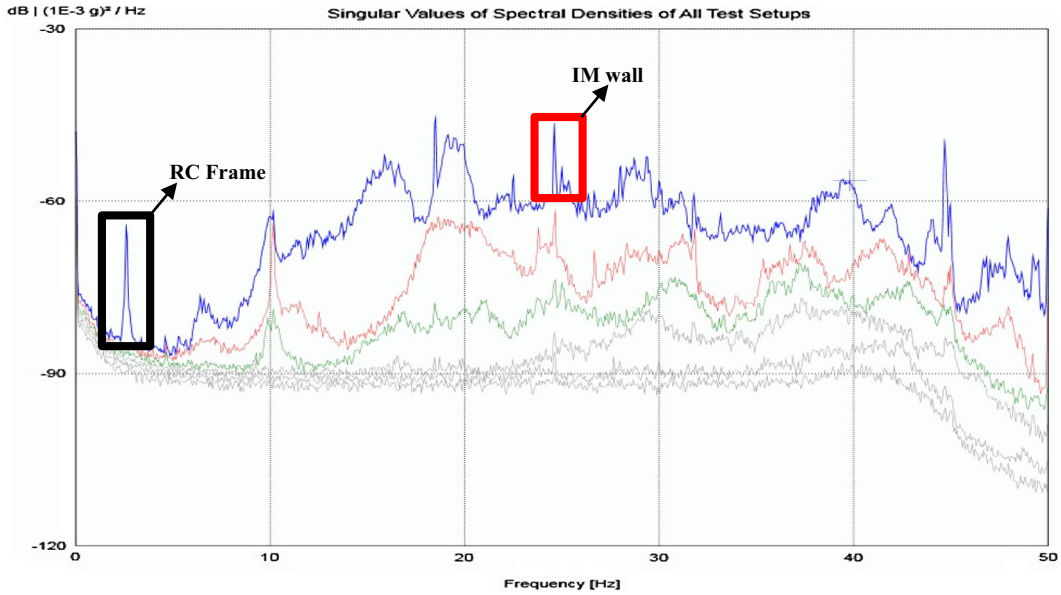

Fig. 8. Modal identification test: identification of the spectral peaks (Black – RC Frame and Red: IM wall). (For interpretation of the references to colour in this figure legend, the reader is referred to the web version of this article.)

where h_{wall} is the panel height), with the main objective of characterizing the evolution of the displacements during the experiment. A significant difference can be seen between the Inf_01 and Inf_02 responses; in the main, displacements of Inf_02 are concentrated in the middle of the wall, particularly focusing on the centre alignment, and the Inf_01 displacements are similar along the panel height (see Figs. 16 and 17).

4. Cyclic out-of-plane experimental test of a full-scale double-leaf im wall with previous in-plane damage

Some southern European buildings are RC buildings with double-leaf IM walls on their façades. According to some survey reports, several out-of-plane collapses of external walls have been observed, since there is no connection between the leaves. The use of this type of strategy for building façades is adopted to correct thermal bridges, and to improve the thermal behaviour of the buildings. The study of this type of non-structural element is important in order to develop retrofit solutions that could improve their seismic performance, and, consequently, help in the calibration of numerical models that represent the behaviour of this type of complex non-structural element when subjected to seismic actions. A full-scale double-leaf panel (Inf_03) comprising an external 15 cm thick leaf and an internal 11 cm thick leaf, was added aligned with the internal side of the beam, leaving a hollow thickness of 4 cm. This double-leaf panel was first tested for in-plane cyclic displacements, after which the internal leaf was removed, leaving the external leaf to be tested under the same out-of-plane loading conditions as for panel Inf_02. The in-plane test set-up, instrumentation and loading condition will be described below. The details of the out-of-plane test are as described for the IM wall, Inf_02.

In this section, the main results of the Inf_03 in-plane and out-of-plane tests will be presented, together with the comparison

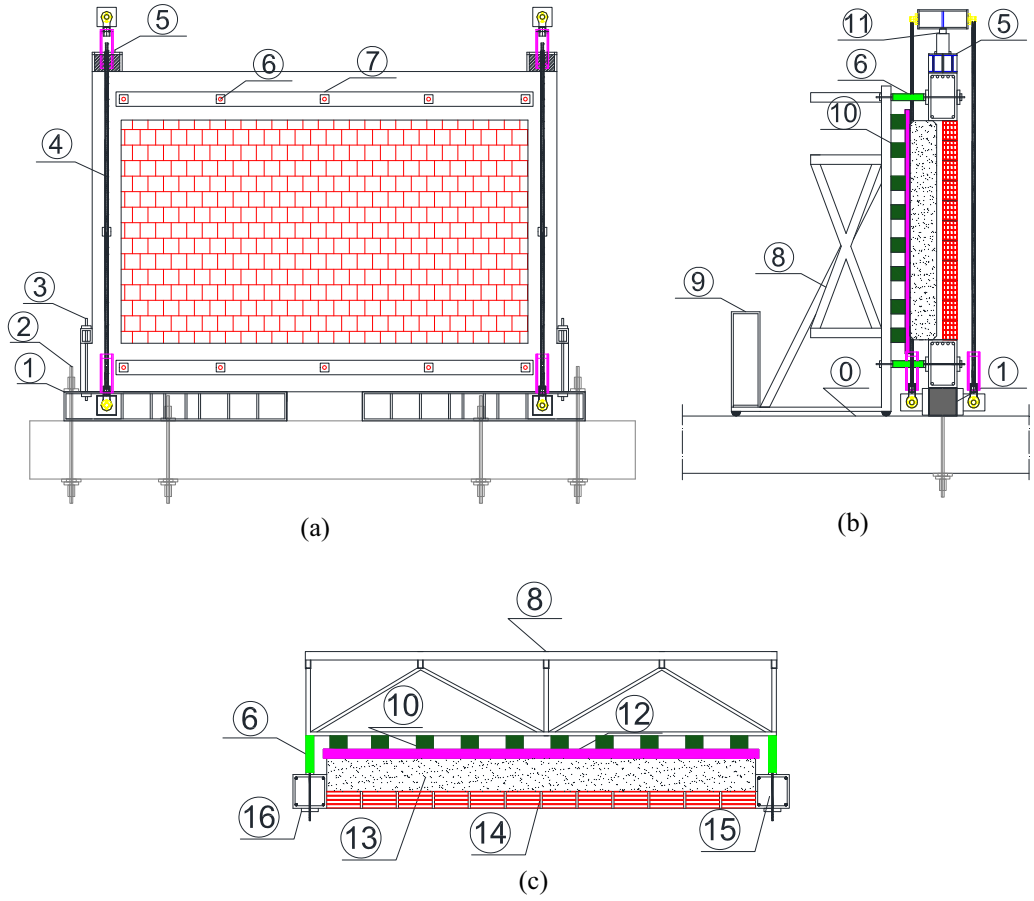

Fig. 9. Layout of the out-of-plane test set-up: (a) front, (b) lateral and (c) plan view. 0 – strong floor, 1 – foundation steel shape, 2 – high-strength rods (∅30 mm) fixing the foundation steel shape to the reaction slab, 3 – steel rod (∅20 mm) connecting the RC frame to the foundation steel shape, 4 – vertical high-strength rods (∅30 mm) to apply axial load, 5 – steel cap, 6 – steel rods (∅20 mm) connecting the RC frame and the reaction structure, 7 – distributing load plate, 8 – self-equilibrated reaction steel structure, 9 – counterweight, 10 – wood bars, 11 – hydraulic jack (for axial load application), 12 – vertical wooden platform, 13 – airbags, 14 – infill panel, 15 – RC column, 16 – steel plate for rod force distribution.

Fig. 10. General view of the out-of-plane experimental test set-up: (a) front view, (b) lateral view.

between the IM walls without previous in-plane damage (Inf_01 and Inf_02) and the Inf_03, with the main objective of evaluating the influence of the in-plane damage in the out-of-plane response of the IM wall.

4.1. In-plane test set-up

The in-plane test consisted of the application of a horizontal force on the top of the RC frame using a servo-controlled hydraulic actuator (±500 kN capacity with ±150 mm stroke) attached to a steel reaction structure (Fig. 18). The horizontal force was transmitted to the RC frame by two high strength rods (∅22 mm) (in the front and rear specimen sides) tying two steel shapes at the left and right extremities of the top beam (Fig. 19), in order to apply in-plane loading cycle reversals. The two high strength rods were linked at 1/4, 1/2 and 3/4 of the beam length to steel plates that connect with the corresponding one of the other side of the beam by 2 steel rods (∅10 mm) with the main objective of mobilize and

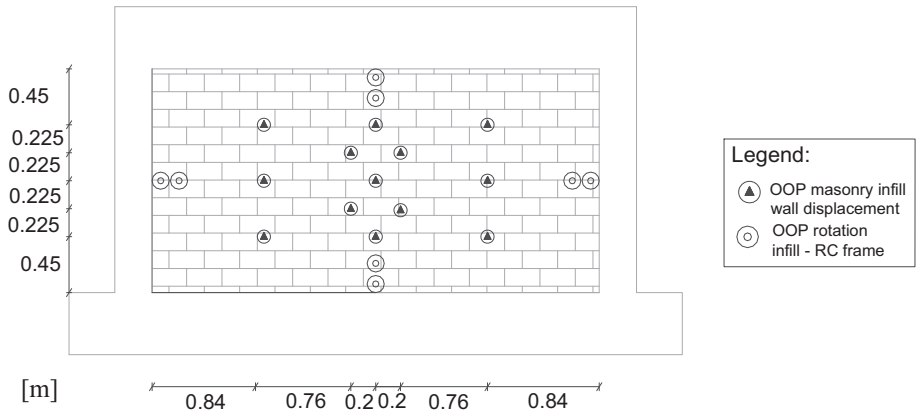

Fig. 11. Layout of the out-of-plane test instrumentation (in m).

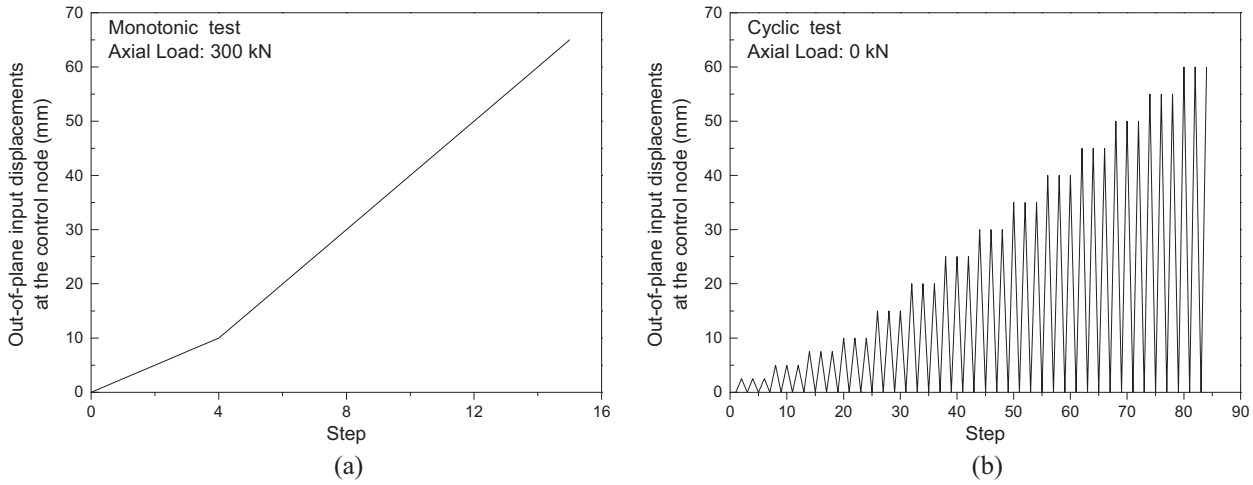

Fig. 12. Loading condition for: (a) monotonic test Inf_01 and (b) cyclic test Inf_02.

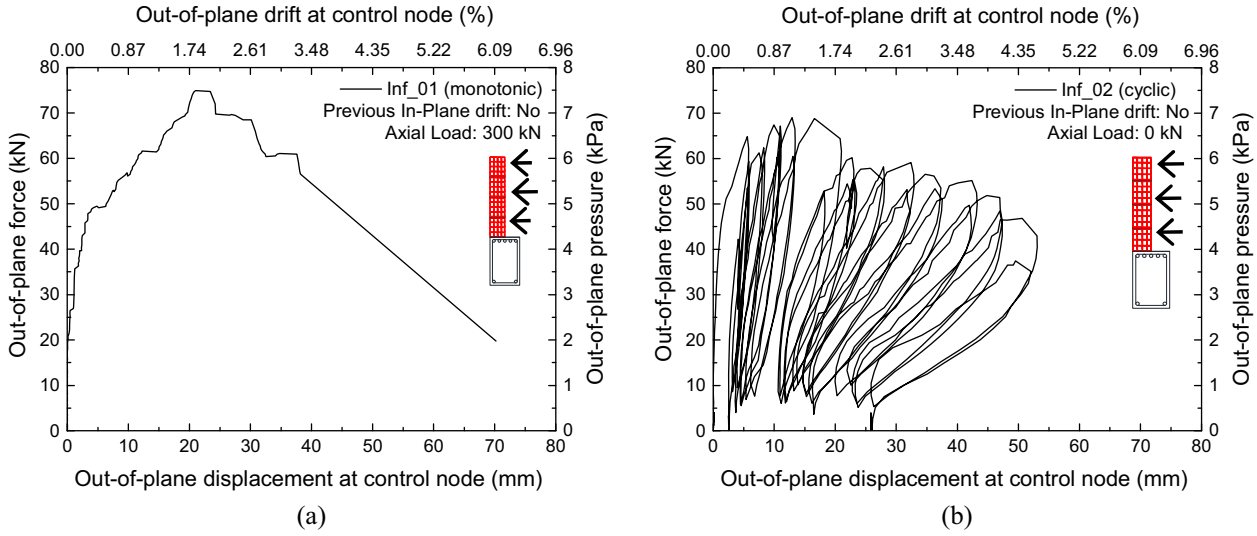

Fig. 13. Out-of-plane force–displacement test results: (a) Inf_01 and (b) Inf_02.

distribute the in-plane load along the entire top beam cross-section uniformly (Fig. 20).

The column axial load was applied using one hydraulic jack per column, attached to the top and bottom of the steel devices by means of high-strength rods with hinged extremities. The in-plane infilled frame was tested under the so-applied column axial load of 300 kN kept constant with the prescribed value measured by load cells attached to the jacks. The test set-up was also

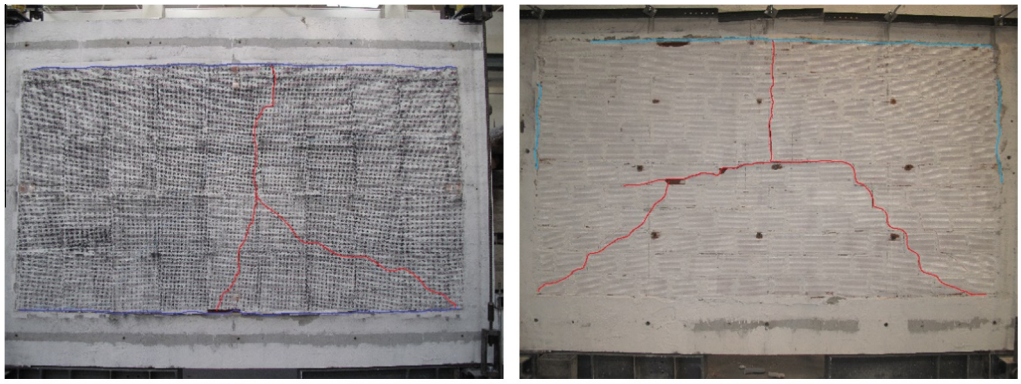

Fig. 14. Out-of-plane observed damage: (a) Inf_01 and (b) Inf_02.

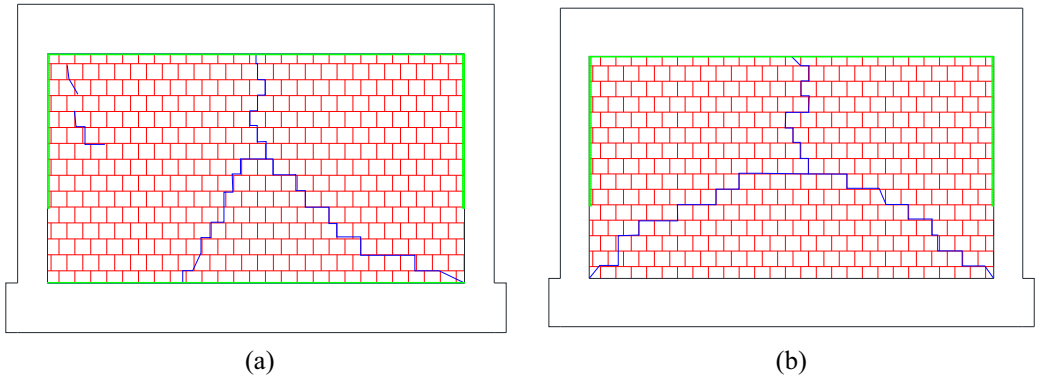

Fig. 15. Cracking pattern: (a) Inf_01 and (b) Inf_02.

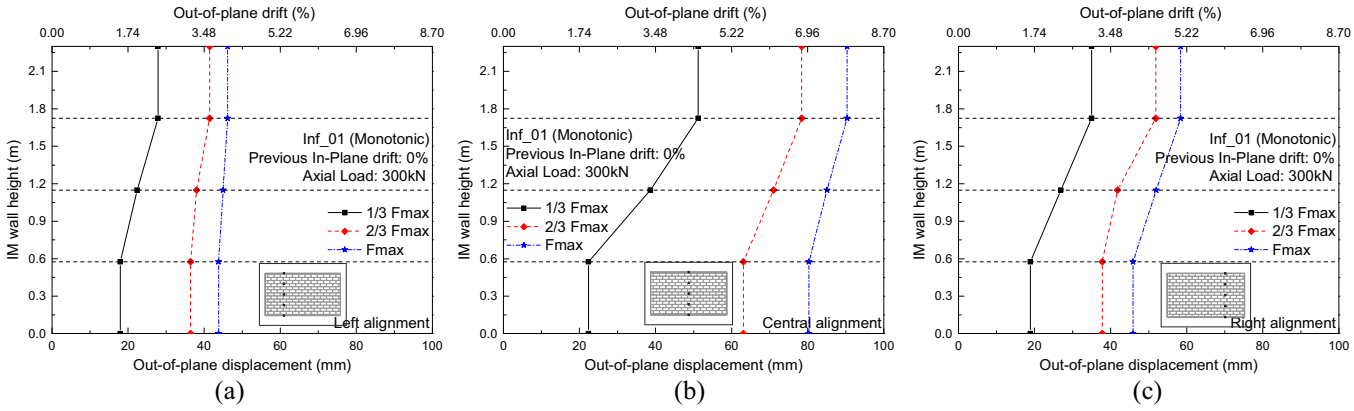

Fig. 16. Out-of-plane displacement profiles of Inf_01: (a) left, (b) central and (c) right alignment.

provided with an additional guiding structure to prevent out-of-plane displacements of the infilled RC frame, while allowing it to slide along the steel shape guides. Fig. 20 shows the layout of the in-plane experimental test set-up, illustrating each element with a corresponding description.

4.2. Instrumentation

The instrumentation of the in-plane tests comprised a total of 21 displacement transducers, both LVDTs and DWTs, as illustrated in Fig. 21. The instrumentation was divided into three different groups according to the corresponding measurement objective: (i) out-of-plane displacements of the infilled RC frame (3 LVDTs); (ii) diagonal displacements in the infill panel and in the RC frame (8 DWTs) in both specimen sides and (iii) in-plane displacements of the infilled RC frame (10 LVDTs).

4.3. Loading condition

As previously stated, the aim of the present experiment is to better understand the in-plane behaviour of IM walls, particularly double-leaf IM walls. To this end, cyclic in-plane displacements were imposed at the top of the IM wall with steadily increasing displacement levels. The in-plane maximum drift was assumed taking into account two premises: (i) the maximum strength of the double leaf infill masonry wall is reached; and (ii) not achieve

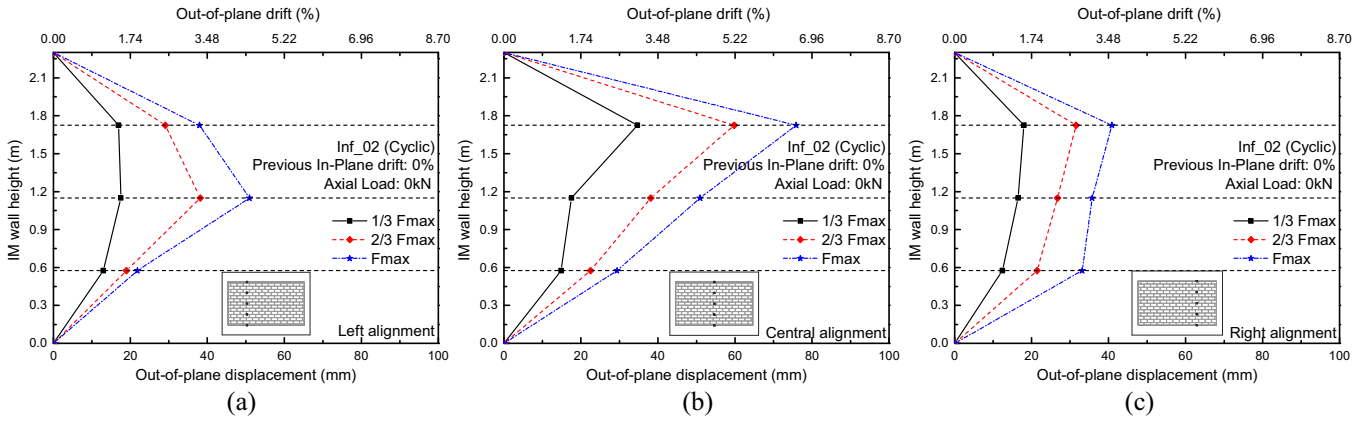

Fig. 17. Out-of-plane displacement profiles of Inf_02: (a) left, (b) central and (c) right alignment.

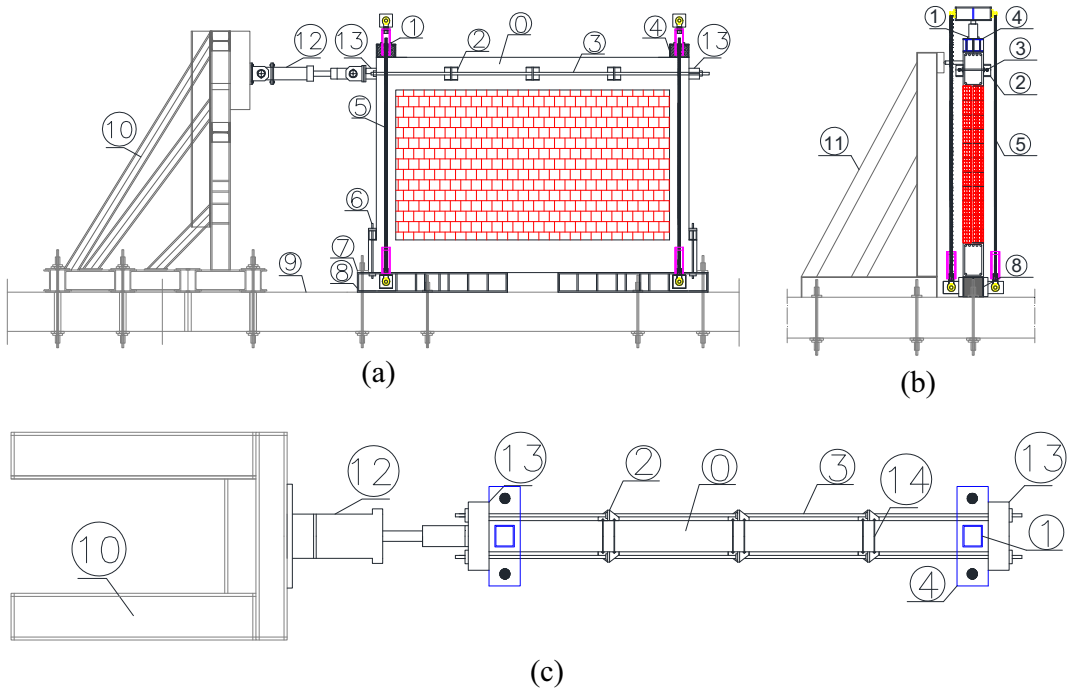

Fig. 18. Layout of the in-plane experimental test set-up: (a) front view; (b) lateral view and (c) Back view. 0 – top beam, 1 – hydraulic jack (for axial load application), 2 – steel plates for horizontal force distribution, 3 – horizontal high-strength rods (∅22 mm), 4 – head steel shape, 5 – vertical high-strength rods (∅30 mm), 6 – steel rod (∅20 mm) connecting the RC frame to the foundation steel shape, 7 – high-strength rods (∅30 mm) fixing the foundation steel shape to the reaction slab, 8 – foundation steel shape, 9 – strong floor, 10 – in-plane reaction frame, 11 – out-of-plane reaction and guiding structure, 12 – servo-controlled hydraulic actuator, 13 – right and left head steel profile and 14 – 5 – transversal rods (∅12 mm).

high levels of damage. In the future different levels of in-plane maximum drift will be performed before the out of plane tests with the main goal of define the interaction curve of the in-plane and out-of-plane capacity of the infill masonry walls. Thus a maximum in-plane drift of 0.5% was defined and the following nominal peak displacement levels (mm) were considered: 2.5, 3.5, 9, 12 and 15, with three cycle repetitions for each displacement level. An axial load of 300 kN was applied and kept constant at the top of each RC column during the experimental test.

4.4. Experimental test results

The experimental results will be presented individually for each test, in terms of shear-drift hysteretic curve, displacement profile, and damage evolution and cracking pattern. Finally, the Inf_03 tests will be compared with the Inf_01 and Inf_02 tests to evaluate the influence of the previous in-plane damage on the experimental response of the infill panel.

4.4.1. Shear-drift hysteretic curve

From the analysis results of the force–displacement hysteretic curve (Fig. 22a) and the in-plane displacement profile (Fig. 22b), the following main observations can be drawn.

- The results between the positive and negative loading direction are non-symmetric, due to the longitudinal extension and slacks of the horizontal high strength rod during the experimental test. For this reason the positive loading will be adopted as the reference.
- A continuous increase was observed in the in-plane strength up to 0.25% drift, after which the strength stabilized until 0.5% drift, though with clear stiffness degradation during the test.

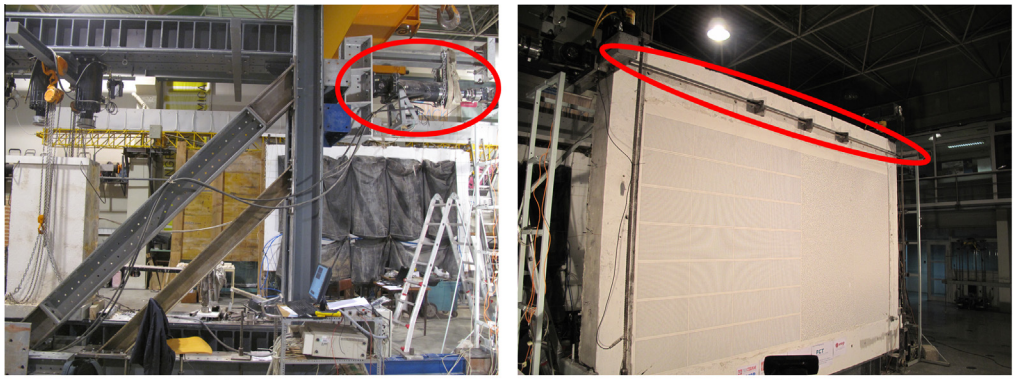

Fig. 19. Detail of: (a) servo-controlled hydraulic actuator (±500 kN capacity with ±150 mm stroke) attached to a reaction steel frame and (b) horizontal high-strength rods (∅30 mm) that are connected to the left and right steel profile placed at mid-height of the top beam.

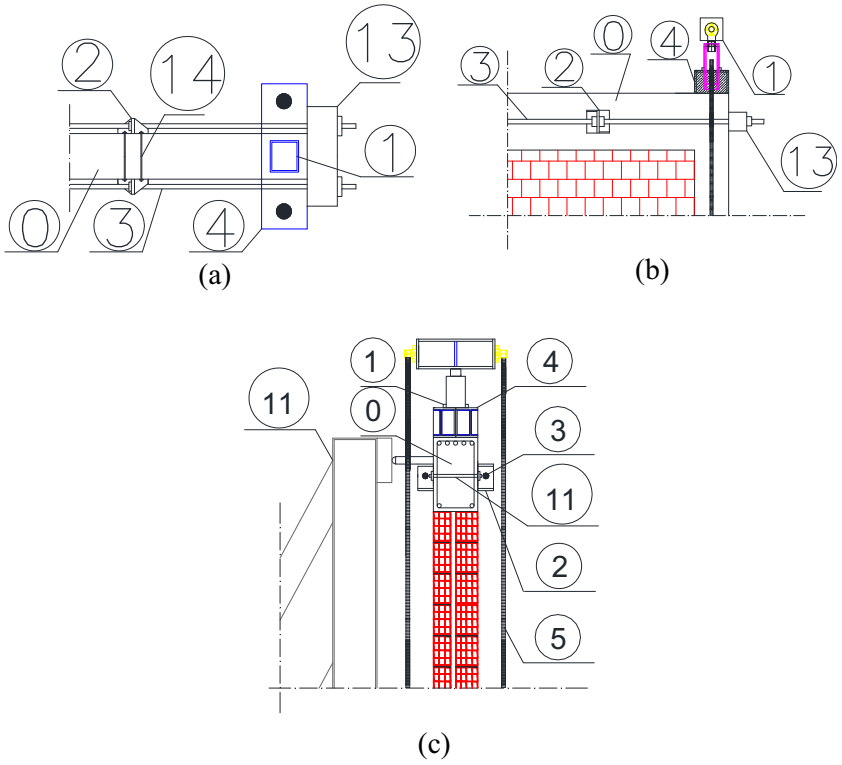

Fig. 20. Detail of the application of horizontal and vertical loading (a) top view; (b) lateral view and (c) transversal view of the upper beam with the particularity.

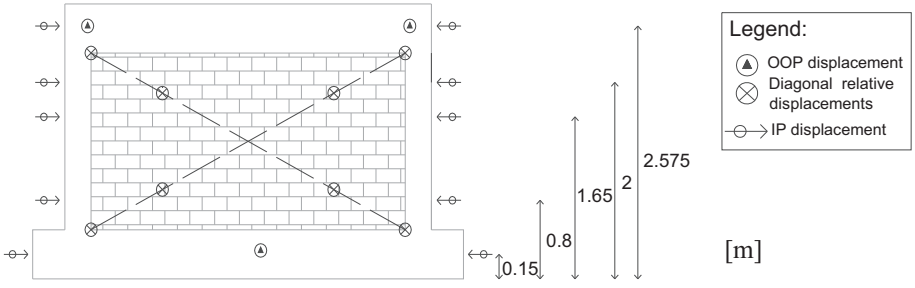

Fig. 21. Layout of the in-plane test instrumentation (in m).

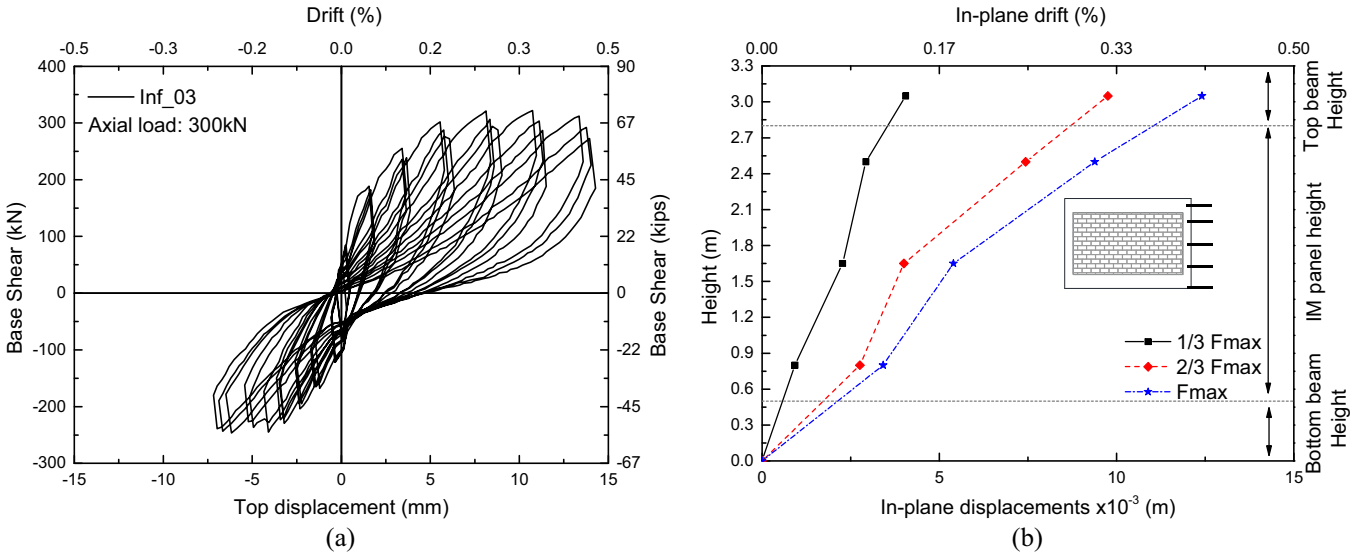

Fig. 22. In-plane test results of Inf_03: (a) force–displacement and (b) in-plane displacement profile.

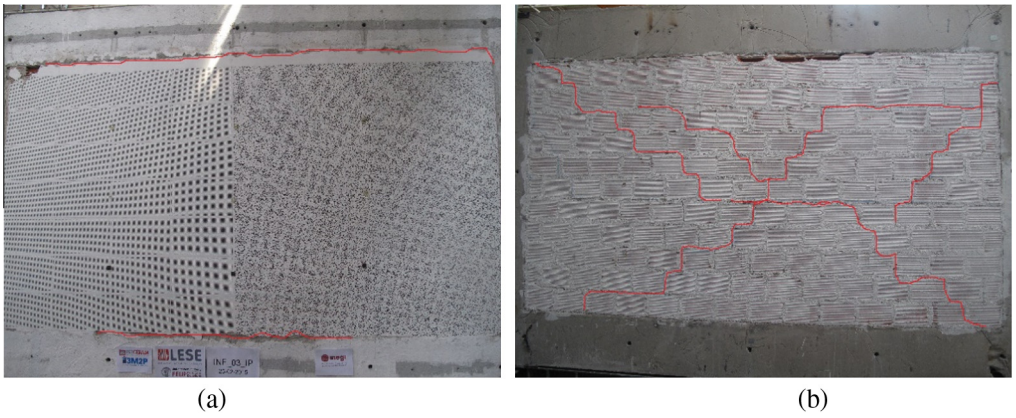

Fig. 23. In-plane test results of Inf_03: (a) front view and (b) back view.

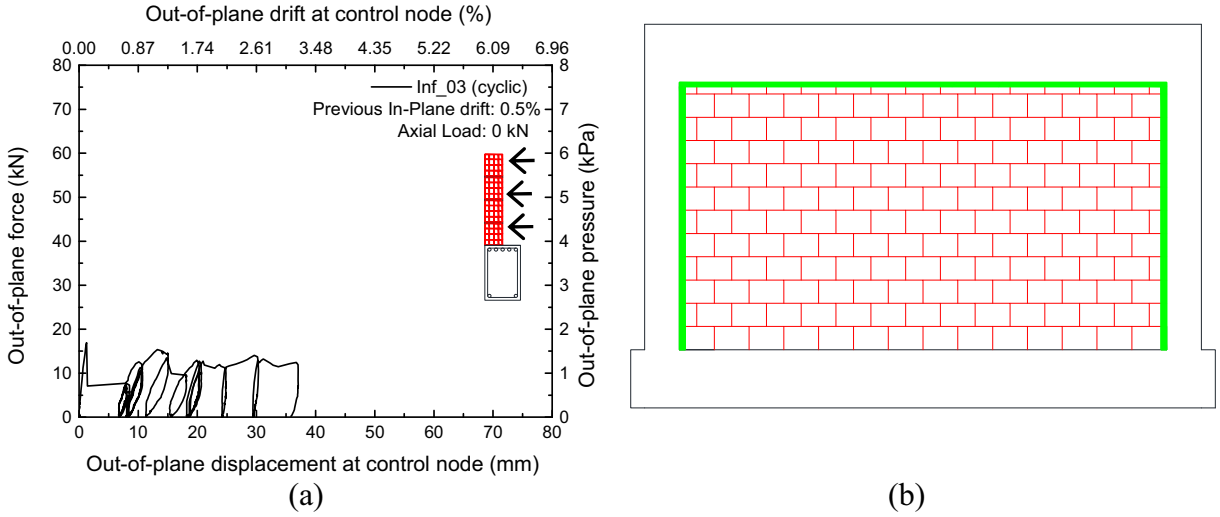

Fig. 24. Out-of-plane test results of Inf_03: (a) force–displacement and (b) crack pattern.

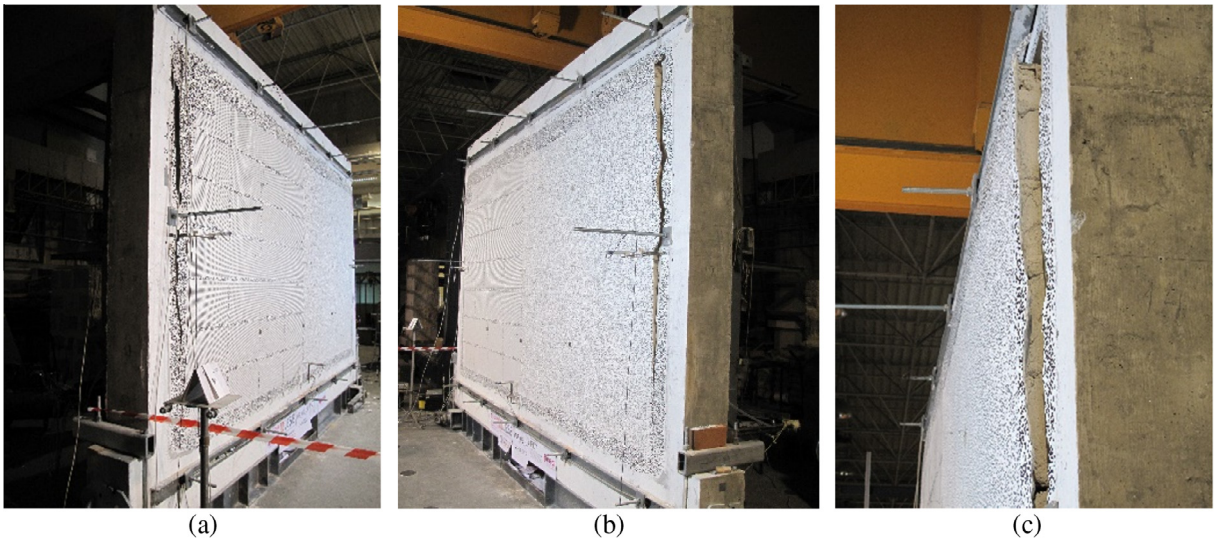

Fig. 25. Inf_03 out-of-plane test damage: (a) left view, (b) right view and (c) zoom of the detachment of the infill panel.

- The maximum strength was characterized by the onset of diagonal cracking in the weaker panel (110 mm thick) and detachment of the surrounding RC frame. At 0.3% drift it was possible to observe panel detachment relative to the top beam and also corner crushing in the stronger panel (Fig. 22).

4.4.2. Damage evolution

During the in-plane experimental test, detachment of the panel from the surrounding RC frame was observed from 0.20% and also corner crushing of the external leaf (Fig. 23a). With regard to the internal leaf, only diagonal cracking was observed and local crushing in the central upper zone of the panel, as illustrated in Fig. 23b.

4.4.3. Out-of-plane test results

Concerning the tests without previous in-plane damage, initial cracking was found for the lower out-of-plane drift values (about 0.1% drift) for the Inf_02 test. The cracking force in both experimental tests was about 50 kN. In the test with previous in-plane damage (Inf_03), initial cracking occurred at 0.1% drift and at a maximum strength of 18 kN, as shown in Fig. 24a. Finally, no cracking pattern occurred in the middle of the IM wall Inf_03, which is related to the observed detachment between the infill panel and the surrounding top beam and columns, evidencing typical rigid body behaviour, as illustrated in Figs. 24b and 25.

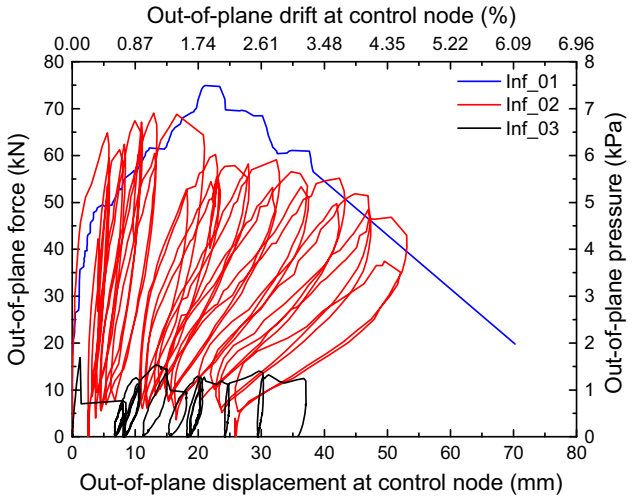

Fig. 27. Global test results: force–displacement.

As in an earthquake, after an in-plane solicitation, shear stresses lead to cracks that tend to separate the masonry wall from the upper and lateral sides of the surrounding RC frame. This tends

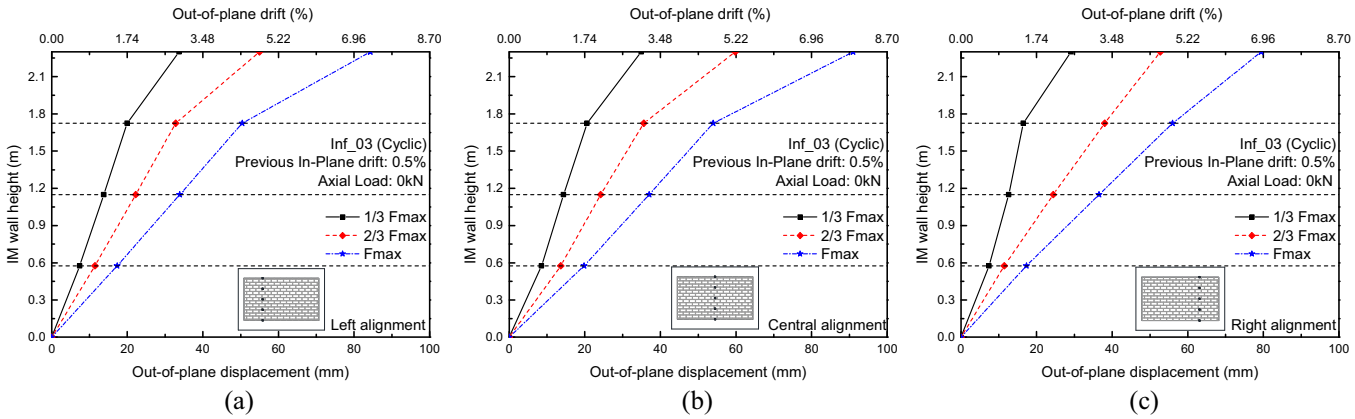

Fig. 26. Inf_03 out-of-plane test result: out-of-plane displacement profiles of (a) left, (b) central and (c) right alignments.

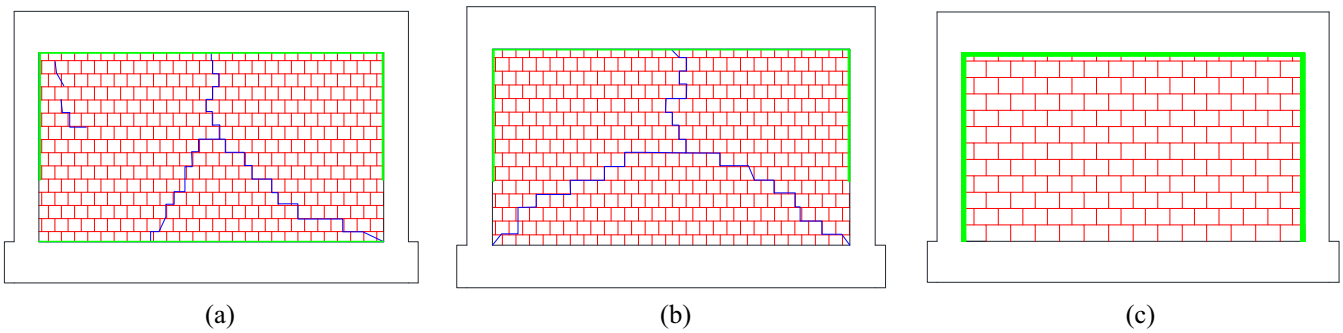

Fig. 28. Global test results cracking pattern: (a) Inf_01, (b) Inf_02 and (c) Inf_03.

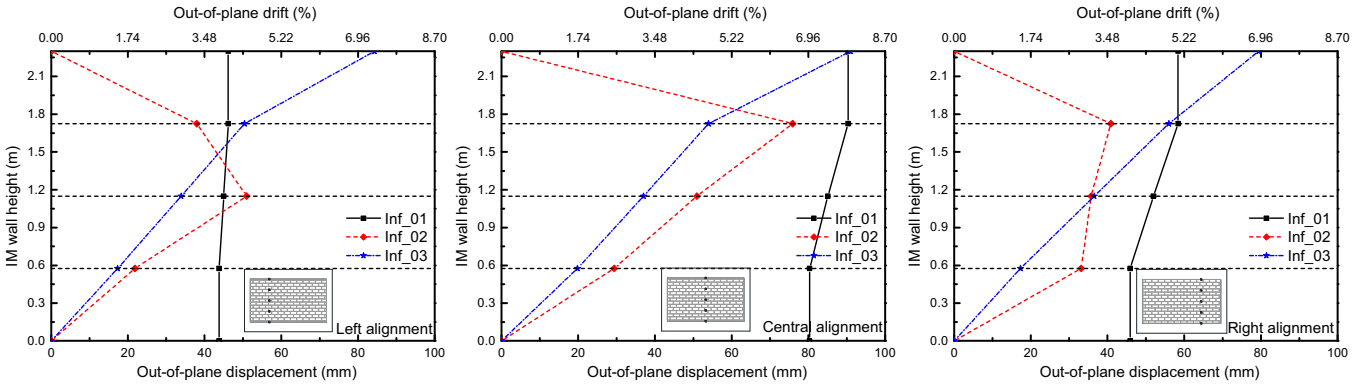

Fig. 29. Global test results out-of-plane displacement profile: (a) Inf_01, (b) Inf_02 and (c) Inf_03.

to reduce the resistance of the wall to the out-of-plane loadings. The out-of-plane displacement profiles show (Fig. 26), as said before, rigid body behaviour.

4.4.4. Global out-of-plane test results

Through comparison between the force–displacement hysteretic curves, a significant difference between the test results, with and without previous in-plane damage can be observed, namely: (a) the maximum strength was almost four times higher for the tests without previous in-plane damage and for higher out-of-plane drift values; (b) the initial stiffness was significantly affected by the introduction of the in-plane damage, that of the test with previous in-plane damage (Inf_03) being almost 30% lower than the original IM walls; (c) a significant maximum strength reduction was found in the tests without the previous in-plane damage, which was not verified in Inf_03 (Fig. 27).

The failure modes observed in each of the tests reveal different out-of-plane behaviour of the IM walls with and without previous in-plane damage. The tests of the original IM walls (Inf_01 and Inf_02) showed vertical cracking, with detachment between the infill panel and the surrounding RC frames in the top and bottom joints. In the Inf_02 wall, trilinear cracking was observed with concentrated deformation in the middle point of the wall, with slight cracking in the top joint. For the test with previous in-plane damage, only detachment was observed between the infill panel and the surrounding top beam and columns, and typical rigid body behaviour was found (Figs. 28 and 29).

5. Conclusions

This paper reports an experimental campaign carried out at the LESE at the Faculty of Engineering of the University of Porto in order to study the out-of-plane behaviour of IM walls, and the influence of the previous in-plane drift in their out-of-plane response. For this, three full-scale infill panels were constructed and were subjected to out-of-plane monotonic and cyclic loading, with and without previous in-plane drift. The out-of-plane loading was applied by using an innovative structure that was specially constructed to undertake this type of experimental test. The experimental test set-up was presented, including all the instrumentation and loading conditions.

A significant difference was found between the test results, with and without previous in-plane damage, namely: (a) the maximum strength was almost four times higher for the tests without previous in-plane damage and for higher out-of-plane drift values; (b) a significant reduction in the initial stiffness was observed in the test with previous in-plane damage when compared with the others; (c) a significant maximum strength reduction was found in the tests without the previous in-plane damage, which was not verified in Inf_03.

The failure modes observed in each of the tests reveal a different out-of-plane behaviour of the IM walls with and without previous in-plane damage. The tests on original IM walls (Inf_01 and Inf_02) showed vertical cracking, with detachment between the infill panel and the surrounding RC frame in the top and bottom joints. In the Inf_02 test wall, trilinear cracking was observed with deformation concentrated in the middle point of the wall, with slight cracking in the top joint. For the test with previous in-plane damage, detachment was observed between the infill panel and the surrounding top beam and columns, and typical rigid body behaviour was found.

Regarding the in-plane test of a full-scale double-leaf IM wall, continuous increase in the in-plane strength up to 0.25% drift was observed, after which the strength stabilized. There was no strength degradation up to 0.5% drift, but clear stiffness degrada-

tion was found during the test. The maximum strength was characterized by a diagonal crack, starting in the weak panel, and detachment relative to the surrounding RC frame, particularly after 0.3% drift when the top beam in both panels became clearly detached and corner crushing was found in the strong panel.

In order to complement the present study and the global findings, experimental tests should be performed in the future according to the following objectives: (i) out-of-plane tests of IM walls with previous in-plane damage for different levels (0.25%, 0.75%, 1%, 1.25% and 1.5% of in-plane drift); (ii) performing similar testing campaign for different IM wall thickness (hollow clay bricks $300 \times 200 \times 110$ mm and $300 \times 200 \times 220$ mm); and finally (iii) out-of-plane tests of IM walls with openings (different sizes and disposition) without and with previous in-plane damage. With this complementary studies the full characterization of original IM walls out-of-plane behaviour will be achieved.

Acknowledgments

The authors would like to acknowledge the technicians of the LESE, Mr. Valdemar Luis and Mr. Nuno Pinto for their support in the experiments reported in this paper, and Preceram for the provision of all the bricks used in the experiments. This experimental research was developed under financial support provided by "FCT – Fundação para a Ciência e Tecnologia", Portugal, namely through the research project PTDC/ECM/122347/2010 – RetroInf – Developing Innovative Solutions for Seismic Retrofitting of Masonry Infill Walls.

References

[1] Fardis M. Experimental and numerical investigations on the seismic response of RC infilled frames and recommendations for code provisions ECOEST/PREC 8. Lisbon: LNEC; 1996.
[2] Dolsek M, Fajfar P. The effect of masonry infills on seismic response of a four storey reinforced concrete frame – a probabilistic assessment. Eng Struct 2008;30:1991–2001.
[3] Ricci P, De Luca F, Verderame G. 6th April 2009 L'Aquila earthquake, Italy: reinforced concrete building performance. Bull Earthq Eng 2011;9:285–305.
[4] Hermanns L, Fraile A, Alarcón E, Álvarez R. Performance of buildings with masonry infill walls during 2011 Lorca earthquake. Bull Earthquake Eng 2014;12:1977–97.
[5] Penna A, Morandi P, Rota M, Manzini C, Porto F, Magenes G. Performance of masonry buildings during the Emilia 2012 earthquakes. Bull Earthquake Eng 2014;12:2255–73.
[6] De Luca F, Verderame G, Goméz-Martinez F, Pérez-Garciía A. The structural role played by masonry infills on RC buildings performances after the 2011 Lorca, Spain, earthquake. Bull Earthquake Eng 2014;12:1999–2026.
[7] Asteris P, Antoniou S, Sophianopoulos D, Chrysostomou C. Mathematical macromodeling of infilled frames: state of the art. J Struct Eng 2011;137:1508–17.
[8] Romão X, Costa AA, Paupério E, Rodrigues H, Vicente R, Varum H, et al. Field observations and interpretation of the structural performance of constructions after the 11 May 2011 Lorca earthquake. Eng Fail Anal 2013;34:670–92.
[9] Vicente R, Rodrigues H, Varum H, Costa A, Silva JM. Performance of masonry enclosure walls: lessons learned from recent earthquakes. Earthquake Eng Eng Vibrat 2012;11.
[10] Paulay T, Priestley MJN. Seismic design of RC and masonry buildings. John Wiley; 1992 [ISBN 0-471-54915-0].
[11] Rodrigues H, Arêde A, Varum H, Costa A. Experimental evaluation of rectangular reinforced concrete column behaviour under biaxial cyclic loading. Earthquake Eng Struct Dynam 2013;42:239–59.
[12] Rodrigues H, Furtado A, Arêde A. Behavior of rectangular reinforced-concrete columns under biaxial cyclic loading and variable axial loads. J Struct Eng 2015.
[13] Alinouri H, Danesh F, Bharam S. Effect of soft-storey mechanism caused by infill elimination on displacement demand in nonlinear static procedure using coefficient method. Struct Des Tall Spec Build 2013;22:1269–309.
[14] Furtado A, Rodrigues H, Arêde A, Varum H. Simplified macro-model for infill masonry walls considering the out-of-plane behaviour. Earthquake Eng Struct Dynam 2015.
[15] Calvi G, Bolognini D. Seismic response of reinforced concrete frames infilled with weakly reinforced masonry panels. J Earthquake Eng 2001;5:153–85.
[16] Hak S, Morandi P, Magenes G. Out-of-plane experimental response of strong masonry infills. In: Presented at the second European conference on earthquake engineering and seismology, Istanbul; 2014.
[17] Akhoundi F, Vasconçelos G, Lourenço P, Palha C, Martins A. Out-of-plane behavior of masonry infill walls. Presented at the 7th international conference on seismology & earthquake engineering, Tehran, Iran; 2015.
[18] Furtado A, Costa C, Arêde A, Rodrigues H. Geometric characterisation of Portuguese RC buildings with masonry infill walls. Euro J Environ Civ Eng 2015:1–16.
[19] NP-EN206. Concrete – specification, performance, production and conformity. European Committee for Standardization; 2000 [Portuguese version].
[20] Tensile testing of mettalic materials – Part 1: Method of test at ambient temperature, N.-E. E. C. f. Standardization; 2006.
[21] NI. National Instruments – LabView Signal Express; 2010.
[22] SVS. Structural Vibration Solution – ARTeMIS Extractor Pro. Release 5.3; 2012.
[23] Griffith M, Vaculik J, Lam N, Wilson J, Lumantarna E. Cyclic testing of unreinforced masonry walls in two-way bending. Earthquake Eng Struct Dynam 2007;36:801–21.
[24] Ferreira T, Costa AA, Arêde A, Gomes A, Costa A. Experimental characterization of the out-of-plane performance of regular stone masonry walls, including test setups and axial load influence. Bull Earthquake Eng 2015;13:2667–92.
[25] NI, National Instruments – LabView software; 2012.